PHYSICAL REVIEW B VOLUME 22, NUMBER 6 15 SEPTEMBER 1980

Infrared absorption in NiO microcrystals

C. Pigenet
Laboratoire de Spectrochimie Infrarouge et Raman, Centre National de la Recherche Scientifique-2, 94320-Thiais, France

F. Fievet
Laboratoire de Chimie des Solides Pulvérulents, Université Paris VII-75005-Paris, France

(Received 16 May 1979)

Infrared spectra in the 350–650 cm^{-1} region of different samples of NiO in a powder of submicronic particles have been analyzed in terms of bulk and surface modes and connected to the size and shape of the particles and to solvent effects. Two surface modes observed for cubic particles in air at 510 and 563 cm^{-1} were interpreted with the cubic shape model, excluding the usual spheric model. For cubes of 1000 Å side an important absorption due to the bulk mode ω_T is observed. For very small particles ($\sim$100 Å) an aggregation effect produces a noticeable absorption at 475 cm^{-1} (in air).

I. INTRODUCTION

The validity of cyclic boundary conditions in crystal dynamics introduced by Born and Von Karman[1] has been discussed by Lederman.[2] More recently, following the experimental result of Berreman,[3] theories for the infrared absorption of ionic-crystal slabs and spheres in the continuum approximation, were developed by Fuchs and Kliewer[4–8] and by Englman and Ruppin.[9–11] They concluded that absorption is possible by bulk modes at frequencies lower than ω_T and higher than ω_L—the transverse optical and longitudinal optical bulk modes—and, for small crystals, by surface modes in the ω_T–ω_L gap. In the limit of a very small crystal, that is to say a crystal dimension much smaller than the infrared wavelength, we have only very few solutions in the ω_T–ω_L gap.

Microscopic dynamical models were used in more recent theoretical work[12–14] but only Lagarde's paper[13] involves realistic dimensions of 1000 Å. However all these papers predicted a noticeable absorption peak at ω_T as well as a very broad absorption band in the ω_T–ω_L gap for very small crystals.

For a slab geometry, the experimental absorption peaks agree with the calculated frequencies.[3] Experimental confirmation with powder of microcrystals was confronted with important difficulties due to the lack of homogeneity in particle shape and size and also to scattering and aggregation effects. Most data were obtained with MgO material.[12,13,15,16] The crystals generally had a cubic shape so the lack of agreement between the experimental main band [558 cm^{-1}(Ref. 15)] and that predicted from the usual spherical model ($\omega_F = 605$ cm^{-1}) was not surprising. The spherical model approximation in shape was made in the NiO microcrystal study in Hunt *et al.*[17]

In the present work, we have used NiO obtained by dehydration of $Ni(OH)_2$ under specific and reproductible conditions that yield roughly homogeneous particle shapes and sizes, as we have verified by electron microscopy. We have studied NiO particles of submicronic dimension in which surface modes are dominant and for which the macroscopic theory predicts very simplified solutions; that is a case different from the larger NiO particles studied by Nahum and Ruppin.[18]

We have also observed infrared spectra characteristic of various parallelepipeds and particularly of cubic particles.

II. EXPERIMENTAL METHODS

A. Sample preparation and description

Following an electron-microscopy study of various samples, we have chosen to describe in detail the results from three samples with particularly homogenous particle shapes and sizes and with shapes close to the slab, parallelepiped, and cube geometries (Fig. 1).

These samples were prepared as follows (see also Ref. 19–21):

Sample 1 (the slab geometry) has been obtained from a well-crystallized $Ni(OH)_2$ sample. This hydroxide was obtained in two steps: first, a turbostratic hydroxide precipitate was made (see sample 3 preparation). Then using the precipitate, a well-crystallized hydroxide powder was obtained through isothermal growth at 200 °C for a period of four hours.

The hydroxide was then heated in a weak air

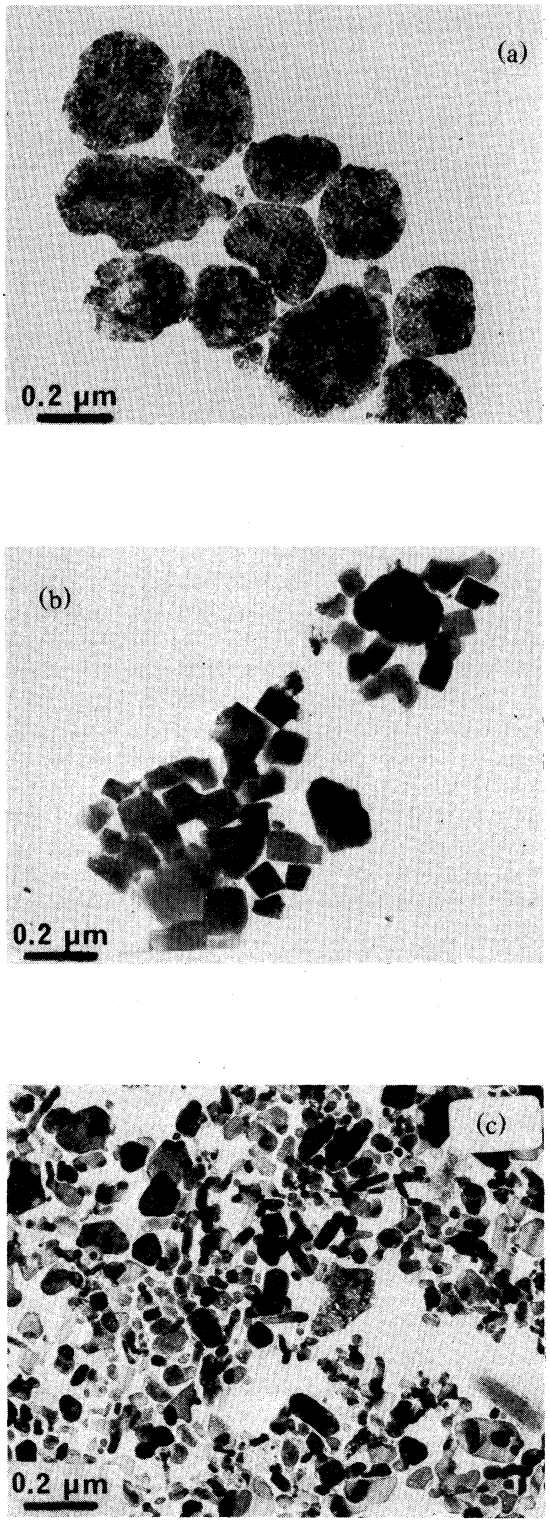

FIG. 1. Electron micrograph of NiO samples: Sample 1 (a), sample 2 (b), and sample 3 (c) (×50 000).

stream with a heating rate of 5° C/h up to 350° C and kept 50 h at this temperature. The particles appear by electron microscopy [Fig. 1(a)] as thin platelets with a (111) orientation. The diameter varies from 2000 to 6000 Å and the thickness from 200 to 400 Å.

Sample 2 (the cubic geometry) was obtained from a well-crystallized hydroxide powder, made as described above and heated in a weak air stream with a heating rate of 150 °C/h up to 950 °C. The particles appear by electron microscopy [Fig. 1 (b)] as round-cornered cubes with edge dimensions varying from 1000 to 2000 Å.

Sample 3 (the parallelepiped geometry) was obtained from a turbostratic hydroxide prepared by mixing a 1-M $Ni(NO_3)_2$ solution and a 20–30% NH_3 solution. The turbostratic hydroxide was obtained through a 3000 rotations/min centrifugation. This hydroxide is heated in a weak air stream with a heating speed of 5 °C/h up to 370 °C and kept 70 h at this temperature. The particles appear [Fig. 1 (c)] as small prisms with a length varying from 100 to 1000 Å and a small edge up 100 to 200 Å, with cube, rod, and slab as limit shapes.

B. Spectroscopic study

The infrared spectra of samples at room and liquid-nitrogen temperatures were obtained on a Perkin Elmer 180 spectrophotometer. The studied samples are embedded in different host media: air, nujol, and cesium iodide. The dielectric constants of these media for infrared frequencies have the following values:

$$\epsilon_M(\text{air}) = 1, \quad \epsilon_M(\text{nujol}) = 1.96 \ ,$$

and

$$\epsilon_M(\text{CsI}) = 3.02 \ .$$

We obtained an air-host medium by evaporation of an alcoholic suspension of NiO powder on a CsI plate, a nujol-host medium with NiO powder mull in nujol between two CsI windows, and a CsI-host medium by pellets of NiO powder mixed with CsI powder.

III. RESULTS AND DISCUSSION

A. General considerations

The structure of NiO is cubic with the space group O_h^5. For a bulk monocrystal there is one infrared active vibrational transverse optical mode $\omega_T = 401 \pm 4$ cm^{-1}.[22] The corresponding longitudinal optical mode was determined by infrared reflection data, using the Lyddane-Sachs-Teller relation, $\omega_L = \omega_T(\epsilon_0/\epsilon_\infty)^{1/2}$, to be at $\omega_L = 580 \pm 2$ cm^{-1} with the values $\epsilon_\infty = 5.7$ and $\epsilon_0 = 11.75$.[22] This result agrees with Raman[23,24] and neutron[25–28] studies.

TABLE I. Calculated frequencies (calculated using $\omega_T = 405\ \text{cm}^{-1}$, $\epsilon_0 = 11.75$, and $\epsilon_\infty = 5.7$ for NiO and $\omega_T = 394\ \text{cm}^{-1}$, $\epsilon_0 = 9.42$, and $\epsilon_\infty = 2.95$ for MgO) (in cm^{-1}) of infrared-active modes for various models of microcrystals.

Geometry	Modes[a]	Outer medium host: Air	Nujol	CsI
NiO samples				
Unlimited slab Unlimited rod	$\omega_\parallel$	405	405	405
Flattened ellipsoid ($a = b = 10c$)	$\omega_\parallel$	415	409	408
Parallelepipeds				
Limited rod ($a = b = c/10$)	$\omega_\parallel$	417	411	409
Limited slab ($a = b = 10c$)	$\omega_\parallel$	422	414	411
fcc aggregate	ω_{Ta}	474	453	437
Cube	ω_C	518	489	470
Sphere	ω_F	541	517	499
Cube	ω_C'	568	556	545
Parallelepipeds				
Limited rod	$\omega_\perp$	568	556	546
Limited slab	$\omega_\perp$	580	579	577
Flattened ellipsoid Unlimited slab Unlimited rod	$\omega_\perp$	581	581	581
MgO samples				
Cube	ω_C	551	501	
Sphere	ω_F	605	554	
Cube	ω_C'	664	634	

[a]For symbols ($\parallel, \perp, \ldots$) meaning, see the text.

In order to analyze each spectrum in detail, we have summarized in Tables I and II the different infrared active mode frequencies expected in the 350–600 cm^{-1} range, taking into account different shape effects, aggregation effects for the different outer media and also two-phonon processes.

1. *Shape effect*

In the continuum approximation the solutions for surface modes are easily obtained for simple geometries such as thin slabs, long cylinders, and small spheres. In the limit of very small dimension (2500 Å for NiO) only three surface modes are expected for an ellipsoidal particle[11] (These modes are formally surface modes in this limit, but also bulk modes in the sense that they describe modes with a uniform polarization over the whole microcrystal in a given direction.); the frequencies ω_i are given by the

TABLE II. Calculated frequencies (in cm^{-1}) of infrared-active two-phonon processes. (Δ, L, Σ are the well-known Brillouin-zone points corresponding to the NiO lattice O_h^5.)

NiO samples		
	LO–TA(Δ) LO–TA(L) LO–TA(Σ)	~350 (medium)
	LA+TA(Δ)	~420 (weak)
	LA+TA(Σ)	~440 (weak)
	LA+TA(Σ)	~490 (weak)
	TO+TA(L) TO+TA(Σ)	~570 (strong)
	TO+TA(Δ)	~600 (medium)
MgO samples		
	TO+TA	~557 (strong)

equation

$$\frac{\omega_i^2}{\omega_T^2} = \frac{\epsilon_0 - \epsilon_M(1-4\pi/N_i)}{\epsilon_\infty - \epsilon_M(1-4\pi/N_i)} ,$$

where N_i is the depolarization constant in the ith principal direction.

For a sphere, the single value $N_i = \frac{4}{3}\pi$ leads to the Fröhlich mode

$$\omega_F = \omega_T \left(\frac{\epsilon_0 + 2\epsilon_M}{\epsilon_\infty + 2\epsilon_M} \right)^{1/2} .$$

For the long cylinder we obtain two modes with polarization parallel to or perpendicular to the axis: $\omega_\parallel = \omega_T$ and

$$\omega_\perp = \omega_T \left(\frac{\epsilon_0 + \epsilon_M}{\epsilon_\infty + \epsilon_M} \right)^{1/2} .$$

For the infinite thin slab we obtain two modes with polarization parallel to or perpendicular to the slab: $\omega_\parallel = \omega_T$ and $\omega_\perp = \omega_L$.

In a recent theoretical paper Langbein[29] has discussed the infrared absorption of small cube and rectangular parallelepipeds in the continuum approximation, using multipole expansion of the external potential. For each shape he obtained specific normal modes. Few modes showed noticeable infrared absorption.

For a cube, the main absorption occurs at a frequency ω_C which is lower than ω_F and which is defined by

$$\frac{\omega_C^2}{\omega_T^2} = \frac{\epsilon_0 + 3.831\epsilon_M}{\epsilon_\infty + 3.831\epsilon_M} .$$

Another weaker absorption occurs at a frequency ω_C' which is higher than ω_F and which is defined by

$$\frac{\omega_C'^2}{\omega_T^2} = \frac{\epsilon_0 + 0.570\epsilon_M}{\epsilon_\infty + 0.570\epsilon_M} .$$

In his paper, Langbein also discusses the theoretical investigations by Van Gelder[30] and by Fuchs[31] on infrared absorption by cubes. Fuchs also finds a strong absorption at a frequency near ω_C but an additional absorption peak occurs at a frequency which is slightly lower than ω_F. The new papers by Fuchs[32] do not modify our previous conclusions. We think that the theory of Langbein provides the best solutions and this is confirmed by our experimental results.

2. *Aggregation effect*

Clippe *et al.*[33] have calculated the dipole-dipole cooperative interaction in various aggregates of NiO spheres with radius $r \leq 1000$ Å and have found additional dipolar absorption peaks with frequencies depending on the geometry of the specific aggregates. A regular fcc aggregate, a good model for a compact aggregate, leads to a transverse mode with a frequency that we call ω_{Ta} which is lower than ω_F and which is defined by

$$\frac{\omega_{Ta}^2}{\omega_F^2} = \frac{1 - \pi(\epsilon_0 - 1)/3\sqrt{2}(\epsilon_0 + 2)}{1 - \pi(\epsilon_\infty - 1)/3\sqrt{2}(\epsilon_\infty + 2)} .$$

3. *Two phonon processes*

In a lattice dynamics approach, Genzel and Martin[12] calculated the phonon density of states for a NiO microcrystal containing on the order of 100 ions and concluded that it was close to that of large crystal, a conclusion corroborated by absorption at the ω_T frequency calculated by Lagarde and Nerenberg[13] for cubes with an edge dimension of 1000 Å.

Consequently, for a very small crystal, we have to consider *a fortiori* the possibility of absorption by harmonics and combinations of short-wavelength phonons present in a large crystal. Lax and Burstein[34] have calculated for O_h^5 ionic crystal a noticeable infrared activity in the $\omega_T - \omega_L$ gap produced by coupling of acoustic and optic short-wavelength phonons through an electric anharmonicity effect, at $\omega \simeq \omega_T\sqrt{2}$.

B. Analysis of spectra

Figure 2 shows infrared transmission spectra of NiO samples embedded in air, nujol, and CsI.

We observe an important variation of spectra for the three samples in the $\omega_T - \omega_L$ range, as expected from the shape effect, as well as a dependence on different host media. The resolution does not improve at low temperature. The remaining variations of shape and size of particles in each sample leads to a distribution of active modes; this distribution, together with scattering, reflection losses, and multiple aggregation effects, gives broad bands.

It must be noted that reflectance peaks at specific frequencies are correlated with absorption peaks at the corresponding frequencies[3,7] and give a decrease in transmittance at the same frequencies for light incident on oriented films at normal incidence. But for a collection of a great number of disordered particles, all reflections add to reduce the apparent transmittance and to increase the width of the region of reduced transmittance, there is not necessarily a good correlation between transmittance and absorptance. However, we can expect that the transmittance varies qualitatively as (1-absorptance).

The observed bands and assignments are given in Table III.

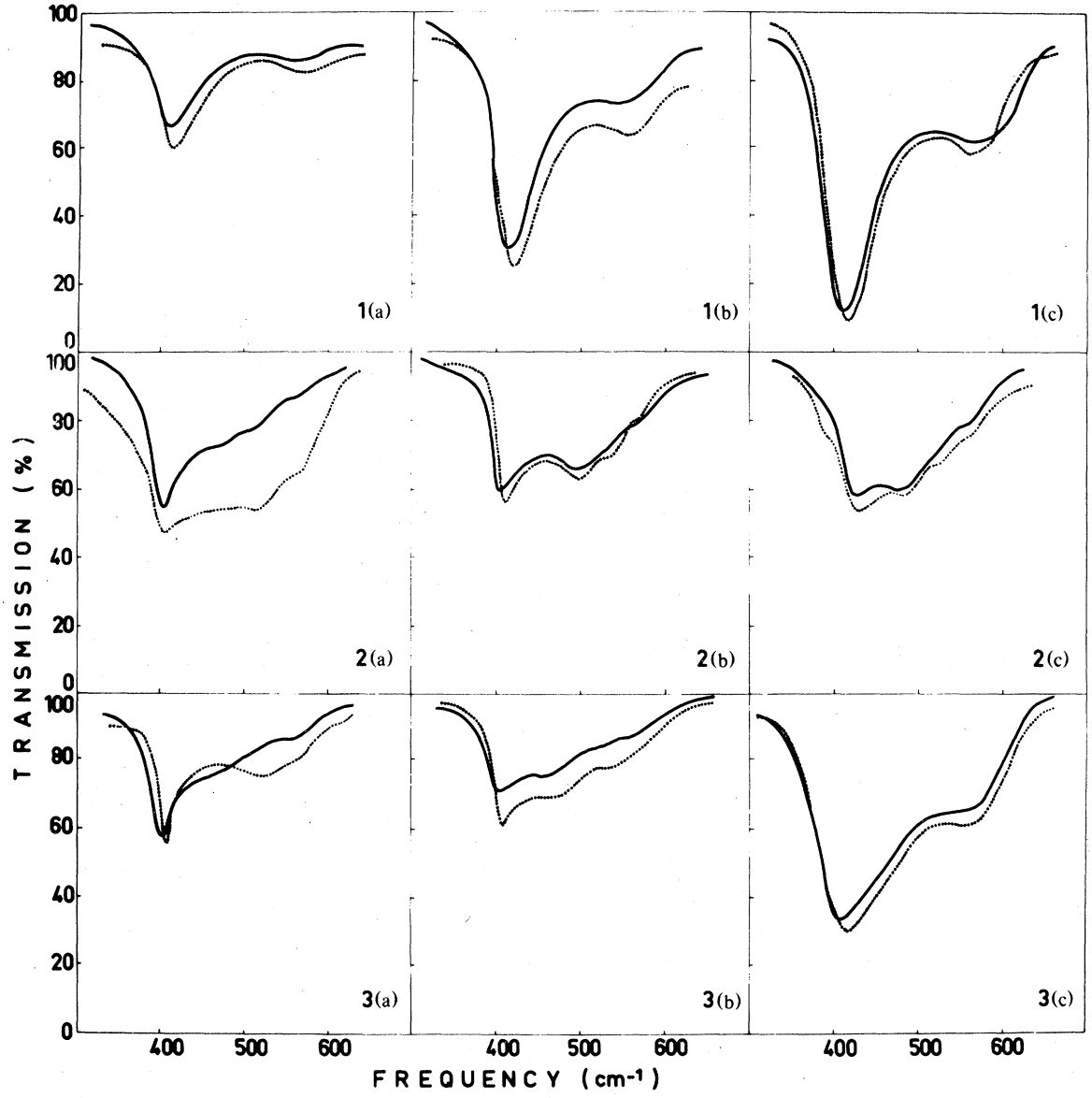

FIG. 2. Infrared spectra of three samples of NiO powder in outer media: (a) air, (b) nujol, and (c) CsI. Full line —— at 300 K. Dotted line . . . . at 100 K.

1. Sample 1

This sample, made up of thin platelets, exhibits a strong absorption at 407 cm^{-1} and a secondary shoulder at ~ 560 cm^{-1} (570 cm^{-1} at 100 K), with positions independent of the host material. These observations are consistent with the thin slab model where two modes are expected: $\omega_{\parallel} \simeq \omega_T$ and $\omega_{\perp} \simeq \omega_L$ without a host effect.

The slight difference between the lower wavelength mode and ω_T may be explained as follows: (a) Sample 1 has a slight lack of stoichiometry ($[Ni^{3+}]/[Ni^{2+}] \leq 0.8\%$) and a lattice parameter ($a = 4.179$ Å) slightly larger than the quasi-perfect-crystal parameter ($a = 4.177$ Å). (b) More probably, the effects of finite platelet length and of curvature of platelet surfaces are to be considered. The calculated values obtained for a very flattened ellipsoidal particle and a flat parallelepiped support this opinion.

Similar considerations must apply to $\omega_{\perp}$, since Dietz *et al.*[23] have observed by Raman scattering a longitudinal mode at 560 cm^{-1} made active through oxygen excess.

In the ω_L region we must also keep in mind an additional absorption due to the two-phonon process at $1.4\omega_T \simeq 570$ cm^{-1}. This was the explanation given

TABLE III. Assignment of observed frequencies (in cm^{-1}). For the symbols ($\parallel$, $\perp$, ...) meaning, see the text.

Host medium	Air		Nujol		CsI		Assignment
Temperatures (K)	300	100	300	100	300	100	
NiO samples							
Sample 1	407	412	410	415	409	414	$\omega_{\parallel}$ of limited slab
	~560	570	550	560	570	560	$\omega_{TA}+\omega_{TO}(L,\Sigma)$
						580	$\omega_{\perp}$ or limited slab
Sample 2	404	405	405	409	~412[a]		ω_T bulk mode
	475		~445[a]		~433[a]		ω_{Ta} compact transverse aggregate mode
	~510	515	492	497	480	490	ω_C cube mode
	563	566	530	534	520	525	ω_C' cube mode
			560	565	560	565	$\omega_{TA}+\omega_{TO}(L,\Sigma)$
Sample 3	402	408	405	410	406[a]		$\omega_{\parallel}$ of limited slab and rod
	~470		460	470	~435[a]		ω_{Ta} compact transverse aggregate mode
	~510	522	~500[a]	~500[a]	~480[a]		ω_C cube mode
			530	540	~520[a]		ω_C' cube mode
	565	570					$\omega_{TA}+\omega_{TO}(L,\Sigma)$
			565	565	565		$\omega_{\perp}$ of limited slab and rod
MgO cubes[b]	400		400				ω_T bulk mode
	558		496				ω_C cube mode
	~670		~620				ω_C' cube mode

[a]For an overlapped band, frequency estimated from absorbance sum.
[b]Genzel and Martin (Ref. 15).

for the side band of a large MgO crystal[34]; a similar side band was observed on a large NiO crystal by Gielisse.[22]

We have no experimental arguments in the slab model, regarding the formal distinction between surface modes of uniform polarization over the whole particle, and bulk modes, ω_T and ω_L. For this model, without dissipative effects, the harmonic surface modes are nonradiative and we can observe only the bulk radiative modes.[4,6,7] But in the thin slab limit we also have absorption at ω_T and ω_L due to bulk modes of polarization parallel and perpendicular to the slab. Thus, an identification of the observed structure as due specifically to bulk or surface modes is not possible.

2. *Sample 2*

This sample, made up to cubic particles, exhibits prominent absorption in the middle of the gap $\omega_T-\omega_L$, as expected for very small cubes, but there also is an absorption peak at 404 $cm^{-1} \simeq \omega_T$.

The band at 404 cm^{-1} in air does not shift in nujol and is assigned to bulk transverse modes. A bulk mode ω_T was observed with MgO cubes of 1000 Å side by Genzel and Martin[15] and a corresponding important absorption peak calculated by Lagarde and Nerenberg.[13] So far as the bulk mode activity is concerned there is a contradiction between the lattice dynamical approach and the macroscopic theory using the dielectric approximation ($c=\infty$, $\vec{\Delta}\times\vec{E}=0$). But if retardation is included we can compare the number of bulk polaritons to the number of surface polaritons using relations given by Englman and Ruppin.[10] They defined a cutoff frequency corresponding to the restriction of long-wavelength modes, and estimated the ratio of bulk polaritons to surface polaritons, in a sphere, to be $6\times10^{-2}N/N_s$, where N is the total number of unit cells and N_s the number of unit cells at the surface. This was qualitatively in agreement with general considerations of Lederman.[2] So, we can estimate that for a diameter larger than 300 Å there are more bulk modes than surface modes. For an ideal sphere, the absorption due to bulk modes is calculated to be very weak at submicronic dimensions,[8,11] but the situation is quite different in a cube with rough faces. The broad band in CsI at 424 cm^{-1} has been resolved into two bands at ~412 and 435 cm^{-1}, the former value being assigned to a bulk mode.

Within the $\omega_T-\omega_L$ gap we observe in air at 300 K

two shoulders at 475 and 510 cm^{-1}. The latter corresponds to absorption at 515 cm^{-1} (at 100 K) and can be related to a band at 492 cm^{-1} in nujol and 480 cm^{-1} in CsI, results compatible with Hunt's observations.[17] These values are much lower than the Fröhlich mode, calculated to lie at 541, 517, and 499 cm^{-1} for the three host media. Nevertheless, Hunt considers a Fröhlich mode assignment possible. Using the function $\epsilon'(\omega)$, the real part of the complex dielectric constant $\epsilon = \epsilon' + i\epsilon''$, given for NiO by Gielisse *et al.*,[22] he obtained from the relation $\epsilon'(\omega_F) = -2$ the value $\omega_F = 510$ cm^{-1} (in the air host medium), which agrees with his observed spectra. But if we use the same function $\epsilon'(\omega)$, with the relation $\epsilon'(\omega_L) = 0$ we obtain for the longitudinal mode a value $\omega_L = 542$ cm^{-1}, as found by Nakagawa,[35] in complete contradiction with other experimental data and the conclusion of Gielisse himself. This is probably due to a lack of precision in the function $\epsilon'(\omega)$ for the resonance.

Interestingly enough, for the well-studied compound MgO, using the data of Jasperse *et al.*,[36] we have a very good agreement between the values $\omega_L = 718$ cm^{-1} determined from the Lyddane-Sachs-Teller relation and $\omega_L = 725$ cm^{-1} determined from the condition $\epsilon' = 0$. Using their data, the relation $\epsilon' = -2$ gives $\omega_F = 605$ cm^{-1}, a value very close to that obtained by the usual equation (Sec. III A *1*): $\omega_F = 598$ cm^{-1}. Here again the main absorption observed on MgO cubes at 558 cm^{-1} (Ref. 15) is noticeably lower.

The frequencies ω_C of the main absorption by surface modes, as predicted in Langbein's paper for a cube in air-, nujol-, or CsI-host medium, are at 518, 489, and 470 cm^{-1}, respectively, in good agreement with the experimental results. Moreover the same mode for an MgO cube in air- or in nujol-host medium leads to the calculated values $\omega_C = 551$ and 501 cm^{-1}, in good agreement with the experimental data: 558 and 498 cm^{-1}.[15]

The weaker bands at 475, 445, and ~ 435 cm^{-1} in air, nujol, and CsI have been explained by a specific aggregate effect. Using the theoretical work of Clippe *et al.*[33] we have calculated a mode occurring at $\omega_{Ta} = 474$, 453, and 437 cm^{-1} for the three host media.

The last shoulder at 563 cm^{-1} in air is assigned to the combined effect of the two-phonon process (570 cm^{-1}) already mentioned and also observed in the other hosts, and of the cubic surface mode ω_C' calculated to be at 568, 556, and 545 cm^{-1} in air, nujol, and CsI. As expected the host effect permits us to observe independently the surface mode ω_C', at 530 cm^{-1} in nujol and 520 cm^{-1} in CsI, and the two phonon process at 560 cm^{-1}. The discrepancy between experimental and theoretical values may be explained by a complex sum of absorbing modes of more or less round-cornered cubes in the interval $\omega_F - \omega_C'$, the Langbein theory already leading to a small absorption at ω_F for the perfect cube. The value $\omega_C' = 664$ cm^{-1} calculated for MgO cubes in air agrees with the shoulder observed at 670 cm^{-1} by Genzel and Martin.[15] Possibly other multiphonon process, given in Table II, can also weakly contribute to the absorption but this second-order effect cannot explain the strong absorption in the gap $\omega_T - \omega_L$.

3. *Sample 3*

This sample is a mixture of very small particles with limit shapes: cubes, slabs, and rods of dimension smaller than 200 Å.

The absorption at a frequency close to ω_T in the three host media is assigned to the mode $\omega_{\parallel}$ of quasiuniform polarization in the larger-dimension direction of rods and slabs. This mode is calculated to be in the interval 405 to 422 cm^{-1} for finite model, with the sample embedded in air, according to Langbein's paper.

At 300 K, in air, a broad and flat shoulder is observed and considered as the sum of absorption at ~ 470 and ~ 510 cm^{-1}. The former corresponds to the conspicuous shoulder at 460 cm^{-1} in nujol and is assigned to the aggregation effect already mentioned. This effect is more important here than in sample 2, since the particles are smaller. At 100 K, in air, the two modes exhibit an inversion of intensity, the mode at 522 cm^{-1} being assigned to the surface mode ω_C, aggregates on the CsI plate being more or less destroyed by the strong lowering of temperature.

The last shoulder at 565 cm^{-1}, in air, is assigned as the sum of the cube mode ω_C', the slab and rod mode $\omega_{\perp}$ corresponding to quasiuniform polarization perpendicular to the larger face, and a two-phonon process. The corresponding modes are observed in nujol. The largest band observed in CsI can be decomposed into several components which are correlated with the nujol data.

IV. CONCLUSIONS

This study of three NiO powder samples clearly shows an important shape effect and also a host effect for particles of submicronic size.

For the cubic shape, the most probable shape of very small particles, we have observed absorption in the $\omega_T - \omega_L$ gap, with a main band ω_C noticeably lower in frequency than the Fröhlich mode ω_F calculated for the sphere model and a weaker band ω_C' higher in frequency than ω_F. These features also appear in the spectra of MgO obtained by Genzel and Martin.[15]

For particles of size 0.1 μm we have observed absorption by the bulk transverse mode ω_T.

With decreasing size an aggregation interaction increases leading to a specific band in the $\omega_T - \omega_C$ interval.

For parallelepipeds having a very small dimension (200 Å) we observe modes at frequencies close to ω_T and ω_L corresponding to modes of quasiuniform polarization, respectively, parallel and perpendicular to the larger face.

[1]M. Born and Th. Von Karman, Phys. Z. 13, 297 (1912); 14, 15 (1913).
[2]W. Lederman, Proc. R. Soc. London Ser. A 182, 362 (1944).
[3]D. W. Berreman, Phys. Rev. 130, 2193 (1963).
[4]R. Fuchs and K. L. Kliewer, Phys. Rev. 140, A2076 (1965).
[5]K. L. Kliewer and R. Fuchs, Phys. Rev. 144, 495 (1966).
[6]K. L. Kliewer and R. Fuchs, Phys. Rev. 150, 573 (1966).
[7]R. Fuchs, K. L. Kliewer, and W. J. Pardee, Phys. Rev. 150, 589 (1966).
[8]R. Fuchs and K. L. Kliewer, J. Opt. Soc. Am. 58, 319 (1968).
[9]R. Englman and R. Ruppin, Phys. Rev. Lett. 16, 898 (1966).
[10]R. Englman and R. Ruppin, J. Phys. C 2, 614 (1968).
[11]R. Ruppin and R. Englman, Rep. Prog. Phys. 33, 149 (1970).
[12]L. Genzel and T. P. Martin, Phys. Status Solidi (b) 51, 101 (1972).
[13]P. Lagarde and M. A. Nerenberg, Phys. Status Solidi (b) 64, 567 (1974).
[14]T. S. Chen, F. W. de Wette, and L. Kleinman, Phys. Rev. B 18, 958 (1978).
[15]L. Genzel and T. P. Martin, Phys. Status Solidi (b) 51, 91 (1972).
[16]J. T. Luxon, D. J. Montgomery, and R. Summitt, Phys. Rev 188, 1345 (1969).
[17]A. J. Hunt, T. R. Steyer, and D. F. Huffman, Surf. Sci. 36, 454 (1973).
[18]J. Nahum and R. Ruppin, Phys. Status Solidi (a) 16, 459 (1973).
[19]F. Fievet and M. Figlarz, J. Catal. 39, 350 (1975).
[20]F. Fievet, P. Germi, F. de Bergerin, and M. Figlarz, J. Appl. Crystallogr. 12, 387 (1979).
[21]F. Fievet, P. Germi, F. de Bergerin, C. Roger, and M. Figlarz, Mater. Res. Bull. 11, 681 (1976).
[22]P. J. Gielisse, J. N. Pendl, L. C. Mansur, R. Marshall, S. S. Mitra, R. Mykolayewycz, and A. Smakula, J. Appl. Phys. 36, 2446 (1965).
[23]R. E. Dietz, G. I. Parisot, and A. E. Meixner, Phys. Rev. B 4, 2302 (1971).
[24]C. H. Perry, E. Anastassakis, and J. Sokoloff, Indian J. Pure Appl. Phys. 9, 930 (1971).
[25]K. S. Upadhyaya and R. K. Singh, J. Phys. Chem. Solids 35, 1175 (1974).
[26]W. Reichardt, V. Wagner, and W. Kress, J. Phys. C 8, 3955 (1955).
[27]R. A. Coy, C. W. Tompson, and E. Gurmen, Solid State Commun. 18, 845 (1976).
[28]R. P. Goyal and S. C. Goyal, Phys. Status Solidi (b) 79, K115 (1977).
[29]D. Langbein, J. Phys. A 9, 627 (1976).
[30]A. P. Van Gelder, J. Holvast, J. H. Stoelinga, and P. Wyder, J. Phys. C 5, 2757 (1972).
[31]R. Fuchs, Phys. Lett. A 48, 353 (1974).
[32]R. Fuchs, Phys. Rev. B 11, 1732 (1975); R. Fuchs, and S. H. Liu, *ibid.* 14, 5521 (1976); R. Fuchs, *ibid.* 18, 7160 (1978).
[33]P. Clippe, R. Evrard, and A. A. Lucas, Phys. Rev. B 14, 1715 (1976).
[34]M. Lax and E. Burstein, Phys. Rev. 97, 39 (1955).
[35]J. Nakagawa, Bull. Chem. Soc. Jpn. 44, 3014 (1971).
[36]R. J. Jasperse, A. Kahan, J. N. Plendl, and S. S. Mitra, Phys. Rev. 146, 526 (1966).

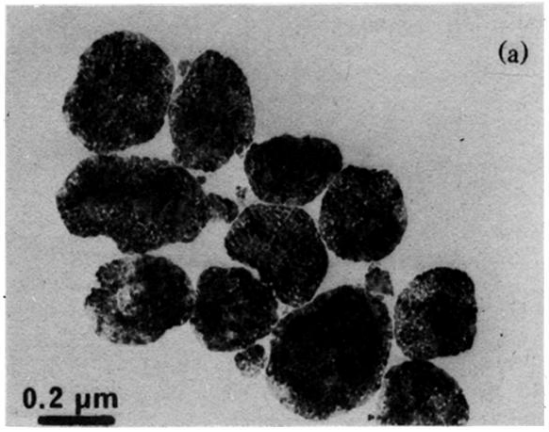

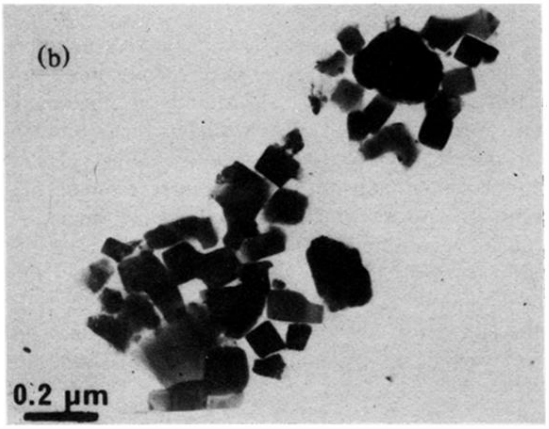

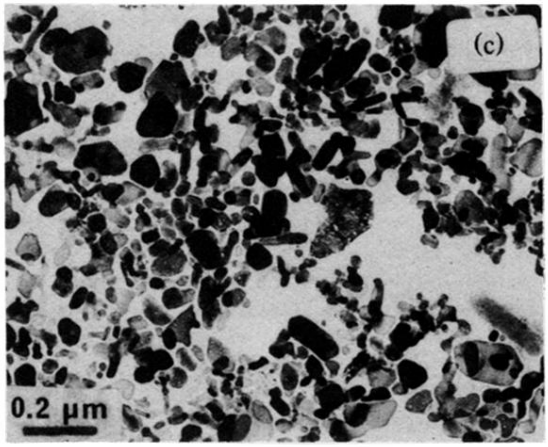

FIG. 1. Electron micrograph of NiO samples: Sample 1 (a), sample 2 (b), and sample 3 (c) (×50 000).